# Re-entrant Arrhythmias and their Control in Models of Mammalian Cardiac Tissue

V.N. Biktashev, Ph.D. and A.V. Holden, Ph.D.

April 15, 1999

**Abstract**

We use detailed biophysical, and simplified models of excitation propagation in heart muscle to study the properties of re-entrant arrhythmias. Using a detailed model of excitation combined with a bidomain description of propagation and action of electric current, we have obtained a theoretical estimation for the defibrillation threshold consistent with experimental data. A series of properly timed low-voltage stimuli can cause directed "resonant" drift of this block, and act as a low-voltage defibrillation strategy. Experimentally observed activation patterns in fibrillating tissue are more complicated than the simplest spiral wave patterns. This is due to complicated geometry, three-dimensional nature of the tissue, its anisotropy and inhomogeneity. However, some fibrillation patterns can be produced by a single re-entrant wave, modulated by inhomogeneous tissue properties and Wenckebach frequency division.

*From School of Biomedical Sciences, Leeds University, Leeds LS2 9JT, UK*

V.N.B. is on leave from: Institute for Mathematical Problems in Biology Pushchino 142292, Russia, and current address is: Department of Applied Mathematics, Leeds University, Leeds LS2 9JT, UK (phone +44-113-2334265)

We use detailed biophysical models from Oxsoft package [1] (rabbit atrium (RA) and guinea pig ventricle (GPV)) and simplified FitzHugh-Nagumo [2, 3] model (FHN) of excitation propagation in heart muscle, to study the properties of re-entrant arrhythmias. The detailed models are able to reproduce realistically quantitative parameters of the re-entrant waves, and the simplified models are used for qualitative study of those waves. The simplest way to describe propagation in tissue is to supplement the equations of the cellular excitability (reaction) with a diffusion of the voltage in a reaction-diffusion system of equations,

$$\begin{aligned} \frac{\partial V}{\partial t} &= -\frac{1}{C} I(V, g_n) + D\nabla^2 V \\ \frac{\partial g_n}{\partial t} &= G(V, g_m) \qquad n, m = 1, \ldots N \end{aligned} \tag{1}$$

where $V$ is transmembrane voltage, $I$ is transmembrane current, $g_n$, $n = 1 \ldots N$ are variables describing state of a cell (ionic concentrations and gating variables of the channels), functions $G$ describe their dynamics and the diffusion coefficient $D$ is chosen to provide appropriate conduction velocity. Fig. 1 illustrates simplest re-entrant waves in two-dimensional tissue — "spiral waves" — in these models. Their periods are close to those observed during experimental atrial and ventricular fibrillation in these animals [4, 5].

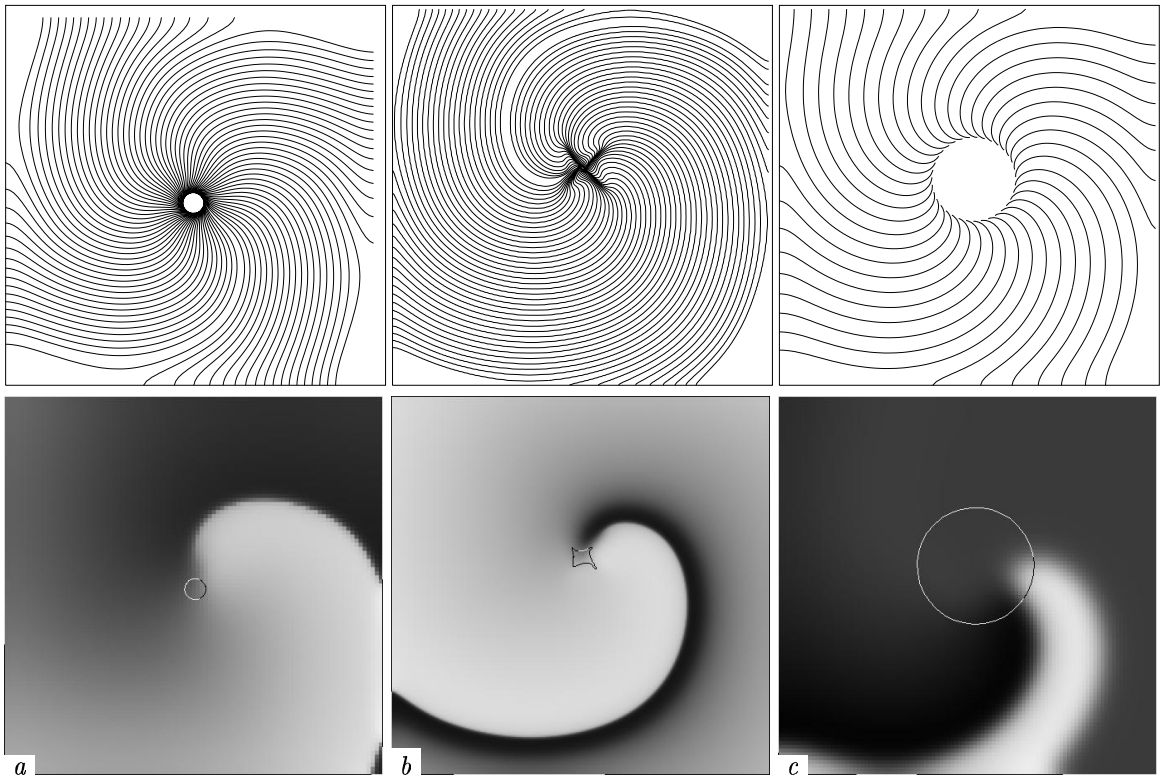


Figure 1: Re-entrant "spiral" waves in biophysically detailed (a) rabbit atrial and (b) guinea pig ventricular (GPV) tissue models from [1] and in (c) FitzHugh-Nagumo (FHN) qualitative model as described in [3], with periods 72 ms, 110 ms and 21 t.u. Top row: isochrone maps; preparation sizes: 30 mm, 30 mm and 25 s.u., time intervals between isochrones: 1 ms, 2 ms and 0.6 t.u. respectively, Bottom row: corresponding snapshots of the spatial distribution of the transmembrane voltage, and trajectory of the tip of the excitation wave during preceding period ("meander patterns").

To describe the effect of electric current stimulation, a bidomain description of the tissue is necessary, which takes into account that electrically, the space of cardiac tissue is separated by the membranes into extracellular and intracellular domains, with different electric properties:

$$\begin{aligned} \nabla(D_e + D_i)\nabla\Phi + \nabla D_i \nabla V &= I_{ext} \\ \frac{\partial V}{\partial t} &= -\frac{1}{C} I(V, g_n) + \nabla D_i \nabla (V + \Phi) \end{aligned}$$

$$\frac{\partial g_n}{\partial t} = G(V, g_m) \quad (2)$$

where $\Phi$ is potential of the extracellular domain, $D_i$ and $D_e$ are intra- and extracellular voltage diffusivity tensors and $I_{ext}$ is external current applied to the tissue. Based on a detailed model of excitation and a bidomain description of the tissue, we have obtained a theoretical estimation for the defibrillation threshold (DFT) consistent with experimental data [6]. Fig. 2 illustrates behaviour of the excitation wave at stimulus amplitude slightly below and slightly above the DFT.

A rough criterion of successful defibrillation is that after the shock, no propagating fronts of excitation should survive in the tissue [7, 8]. The theory of defibrillation suggested in [7, 8, 6] considered that if external current crosses the cellular membrane in one place, it should cross the membrane in the opposite direction elsewhere, *i.e.* have both depolarising and hyperpolarising effects. This is true if the gap junction resistance between the cells is sufficiently large. Alternative theory (see e.g. [9] and references therein) assumes that the gap junction resistance is small, and the action of the electric current is due to inhomogeneities of the extracellular electric field and of the structure of the tissue. In this case the action of the current is maximal in some area around the electrode, called the "virtual electrode", which has been observed experimentally (see *e.g.* [10]). Such localised action of the current can also eliminate re-entrant waves, but the events during this elimination could be more complicated than in the theory of [7, 8, 6]. Fig. 3 illustrates how the virtual electrode generates a new spiral wave, which annihilates with the previously existing spiral wave after three rotations. Using FHN model, such a mechanism has been proposed in [11].

Whatever the details of the action of the electric stimulus onto a spiral wave, if its amplitude is below the defibrillation threshold, then the functional block, or the core of the spiral can be shifted, and so a series of properly timed low-voltage stimuli can cause directed "resonant" drift of this block [12, 13]. The proper timing of the stimuli can be provided by some kind of feed-back using activity recorded at a point [14] or integral activity such as the ECG [15]. As a directed drift can remove the reentrant wave from the excitable tissue by pushing the functional block onto inexcitable boundary, this could be used as a strategy for low-voltage defibrillation. This is illustrated for the monodomain GPV tissue model in Fig. 4.

The ventricular wall of a large mammal is an essentially three-dimensional, with a complicated "rotationally anisotropic" structure, related to the anatomy of the fibres. This structure can be modelled by a spatially-dependent conductivity tensor in both the monodomain description (see Fig. 5), and in the bidomain description.

The behaviour of re-entrant waves in three dimensions can be much more complicated than in two dimensions. For instance, if the conduction block is orientated parallel to the myocardial surfaces, then the surface activation patterns will show ectopic foci rather than classical "spiral-wave" re-entry. Fig. 6 shows this happening in three-dimensional FHN model, and in experimental monomorphic tachycardia in sheep ventricle obtained using a voltage-sensitive dye and optical mapping (for details of experimental procedure see *e.g.* in [16]). If many scroll waves exist in the tissue, then the surface picture can be more complicated [17].

Inhomogeneity of the tissue properties can further complicate the surface patterns. Fig. 7 shows snapshots of experimental fibrillation in sheep ventricle obtained, obtained with the same technique as Fig. 6($a$). The process is so complicated it is difficult to interpret it not only in terms of spiral waves but simply in terms of propagating waves or wavelets. Frequency analysis of activity at different surface points in different experiments has shown that typically in this experimental model of fibrillation, the surface is split onto a few domains, with spectral properties (notably, the dominant frequency) of activity in each domain being uniform, and changing across the domains [18].

The ratio of dominant frequencies of different domains often is ratio of small integers, *i.e.* can be explained by Wenckebach frequency division due to inhomogeneity of tissue properties. Numerical experiment with inhomogeneous FHN model can qualitatively reproduce the frequency domains [19, 20], see Fig. 8.

This interpretation implies that the complicated activity in this experimental model of fibrillation is caused not by many independent re-entrant sources but by one, which is rotating in the region with small refractoriness, and it is inhomogeneity of the tissue that makes the observed activity complicated. This conclusion has a principal importance for the viability of feedback resonant drift as a low voltage defibrillator. Indeed, it would be difficult if not impossible to provide resonance of the external stimulation with all reentrant waves in the tissue. However, if all the activity is caused by one source, it is enough to

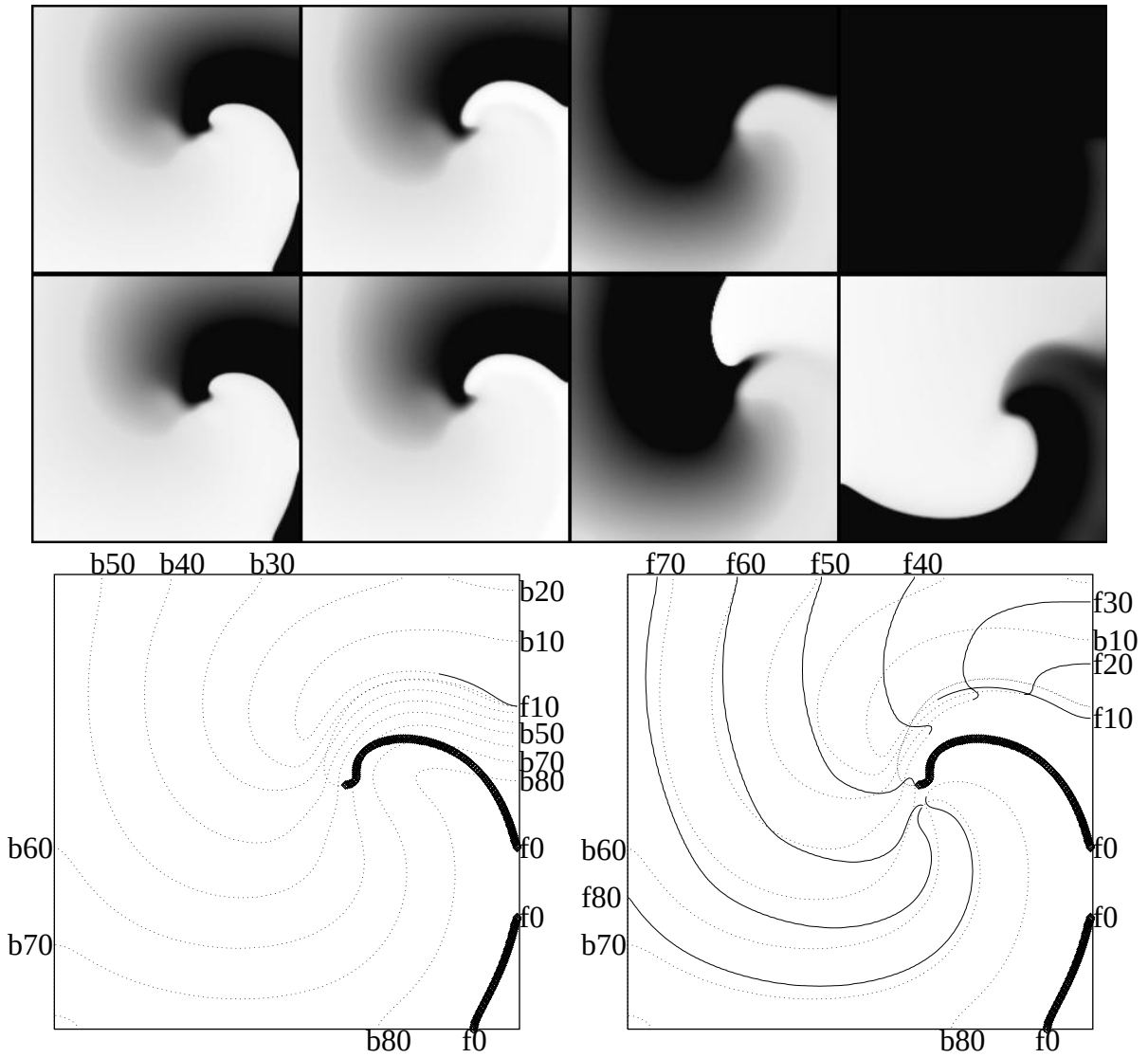


Figure 2: Effect of near-DFT electric shock onto re-entrant wave in a 2D "reaction-diffusion" GPV model. *Top* Snapshots from movies of suprathreshold (above, with 800 nA/cell) and subthreshold (below, with 650 nA/cell) defibrillation by a spatially uniform 2 ms depolarising current pulse $I_{ext}(t)$ of a spiral wave in the GPV simplified bidomain model [6]. Time moments are chosen 0, 3, 40 and 80 ms (left to right) measured since the beginning of the stimulus. *Bottom* Wavefronts (solid lines) and wavebacks (dotted lines) visualised as $V = -10$mV isolines every 10 ms during (left) the suprathreshold and (right) subthreshold defibrillating shocks. The first isoline (front shown by bold line) is just before the defibrillating pulse was applied; the spiral wave is rotating counterclockwise. Labels code the isolines' type (**b**ack and **f**ront) and time in ms since the shock application.

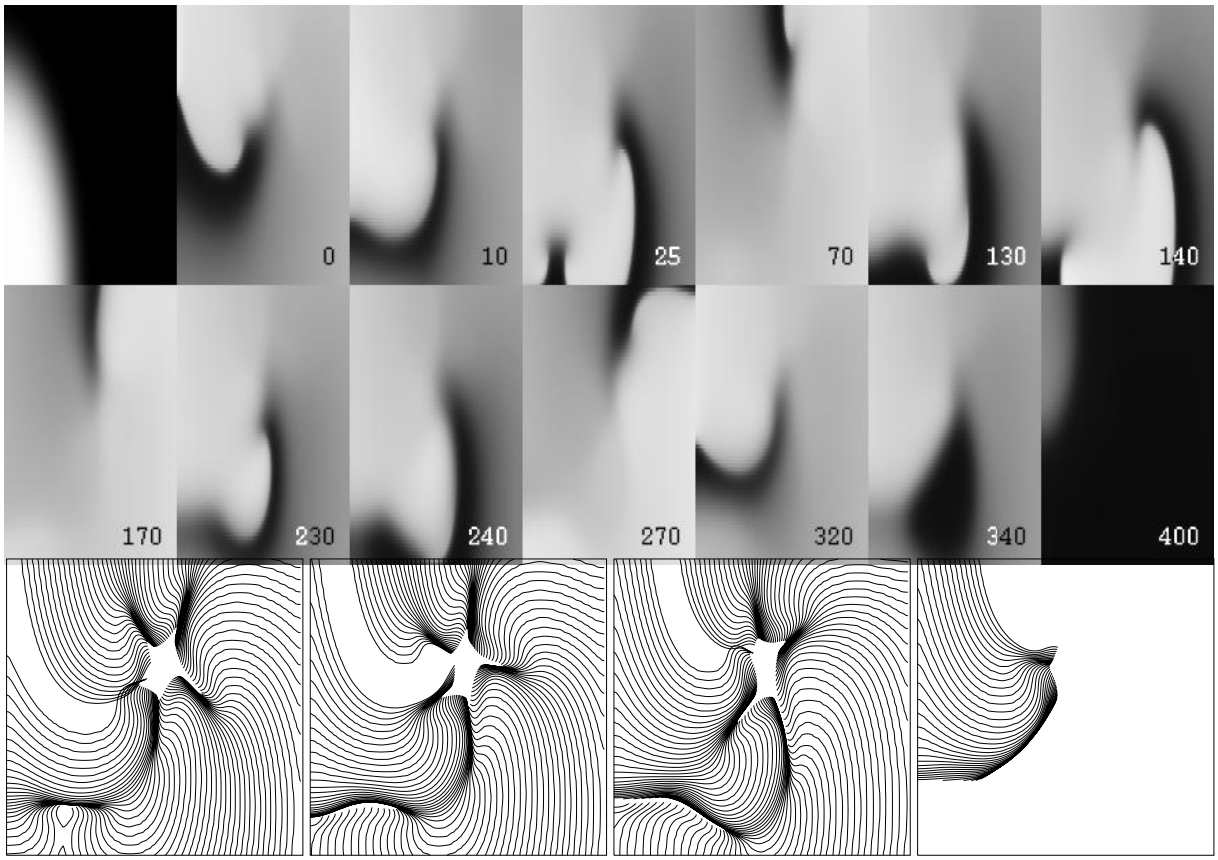


Figure 3: Elimination of a reentrant wave by a "virtual electrode" induced by stimulation of a near-DFT magnitude in full bidomain GPV model. Top: first frame shows the area of the virtual electrode; other frames show distribution of transmembrane voltage at selected time moments. The time is in ms since the beginning of the stimulus. Bottom: four consecutive 100 ms isochrone maps, interval between isochrones 1 ms.

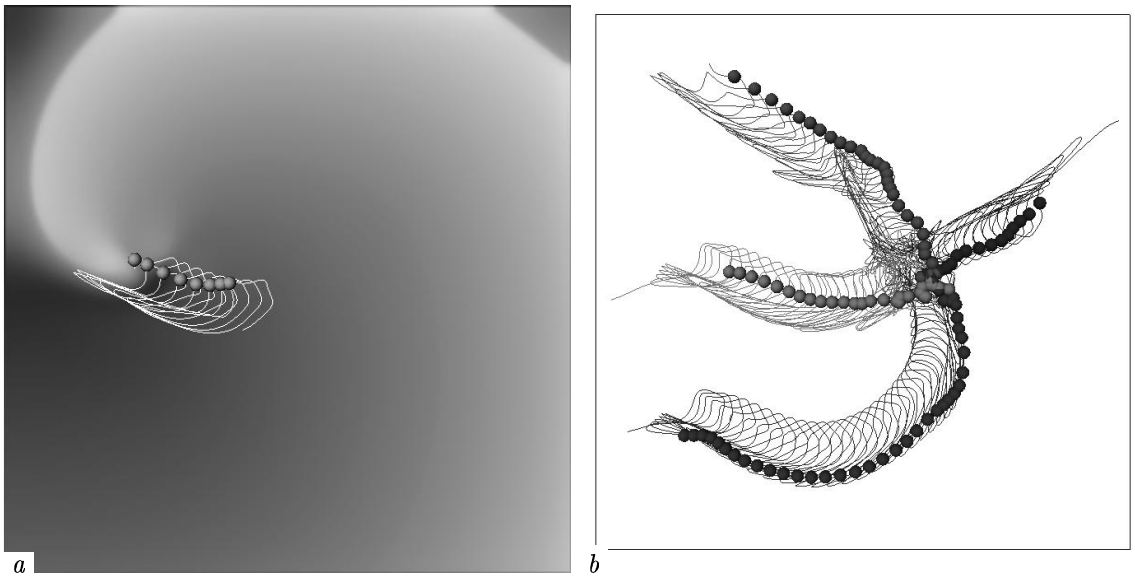


Figure 4: Feed-back driven low-voltage stimulation of a reentrant wave in a 2D monodomain GPV tissue model leads to the directed drift and extinguishing of the wave. ($a$) The spiral wave and the trajectory of its tip during last few rotations. ($b$) Trajectories of the tips of spirals in four numerical experiments, with different delay in the feedback loop. The stimulation was by rectangular current pulses uniformly in space, controlled by feedback via a recording site in the bottom left hand corner of the medium and delays 0, 25, 50 and 75 ms; average period of rotation is between 100 and 110 ms, square size 20 mm. The balls show the tip positions at the beginning of each stimulus. The visible fractures in the trajectories in ($b$) correspond to different phase locks between stimulation and meander.

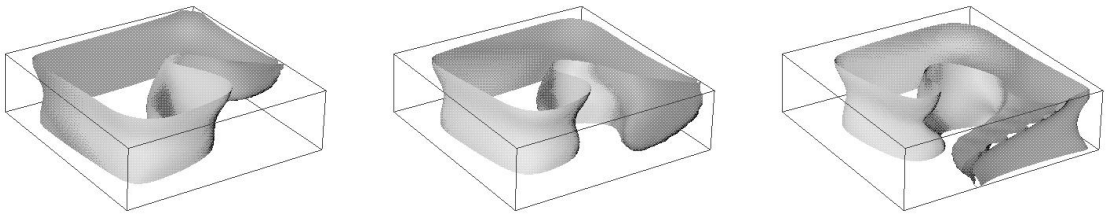

Figure 5: Spiral wave in the monodomain GPV model in thee dimensions with rotational anisotropy of 3:1 velocity ratio and total rotation angle 120°, size of preparation $5 \times 5 \times 1.5$ mm. Interval between snapshots 10 ms.

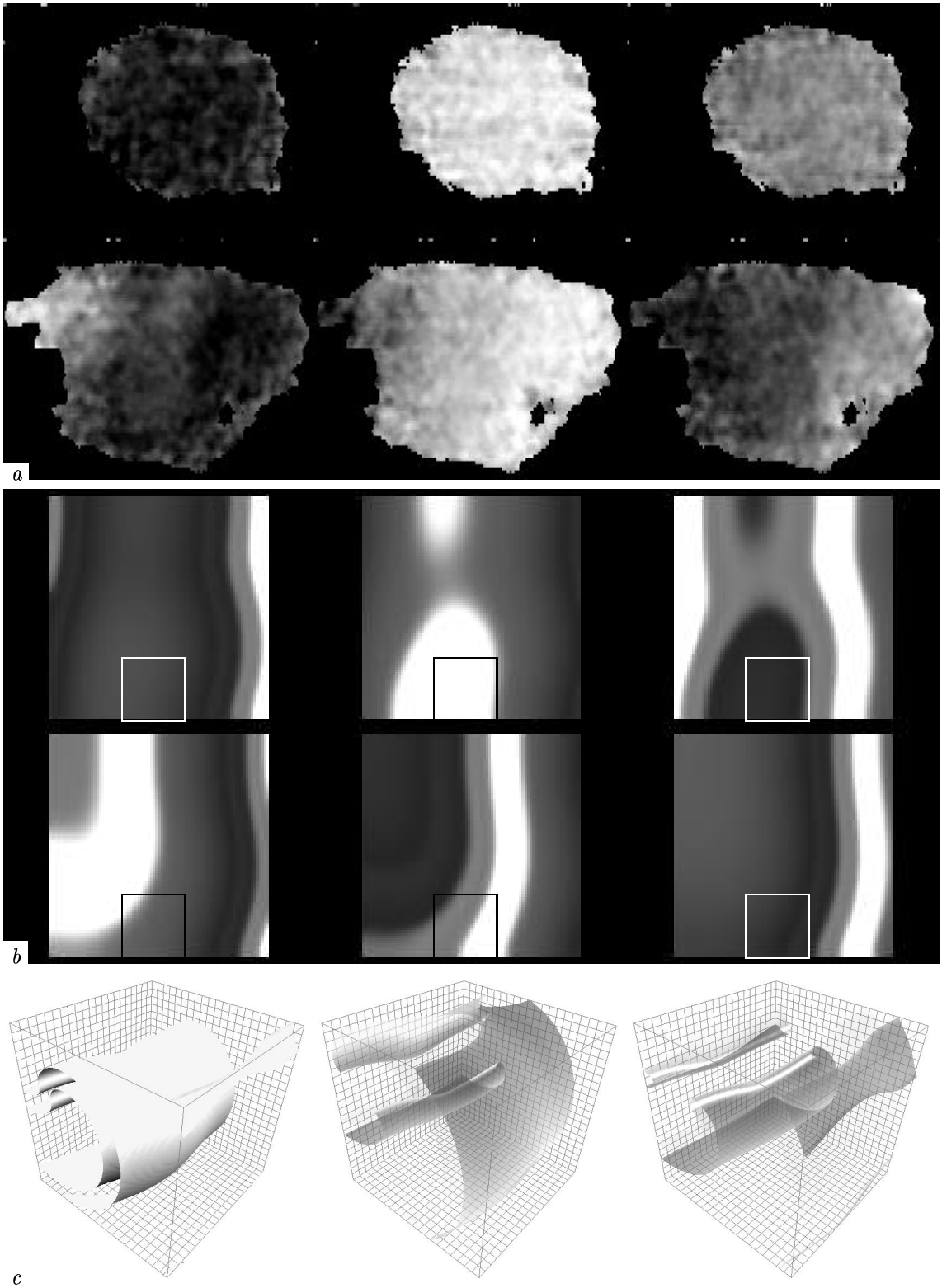


Figure 6: Comparison of experimental surface views of simple excitation pattern ("monomorphic tachycardia") with numerical simulations of metastable double scroll in FHN (medium size $43 \times 43 \times 43$ s.u.). ($a$) experimental patterns, the upper three pictures are epicardial views and the lower three pictures are endocardial views with interval 50 ms. ($b$): numerical simulations, surface patterns. Small squares show the region where the behaviour in the experiment. ($c$): numerical simulations, corresponding volume view.

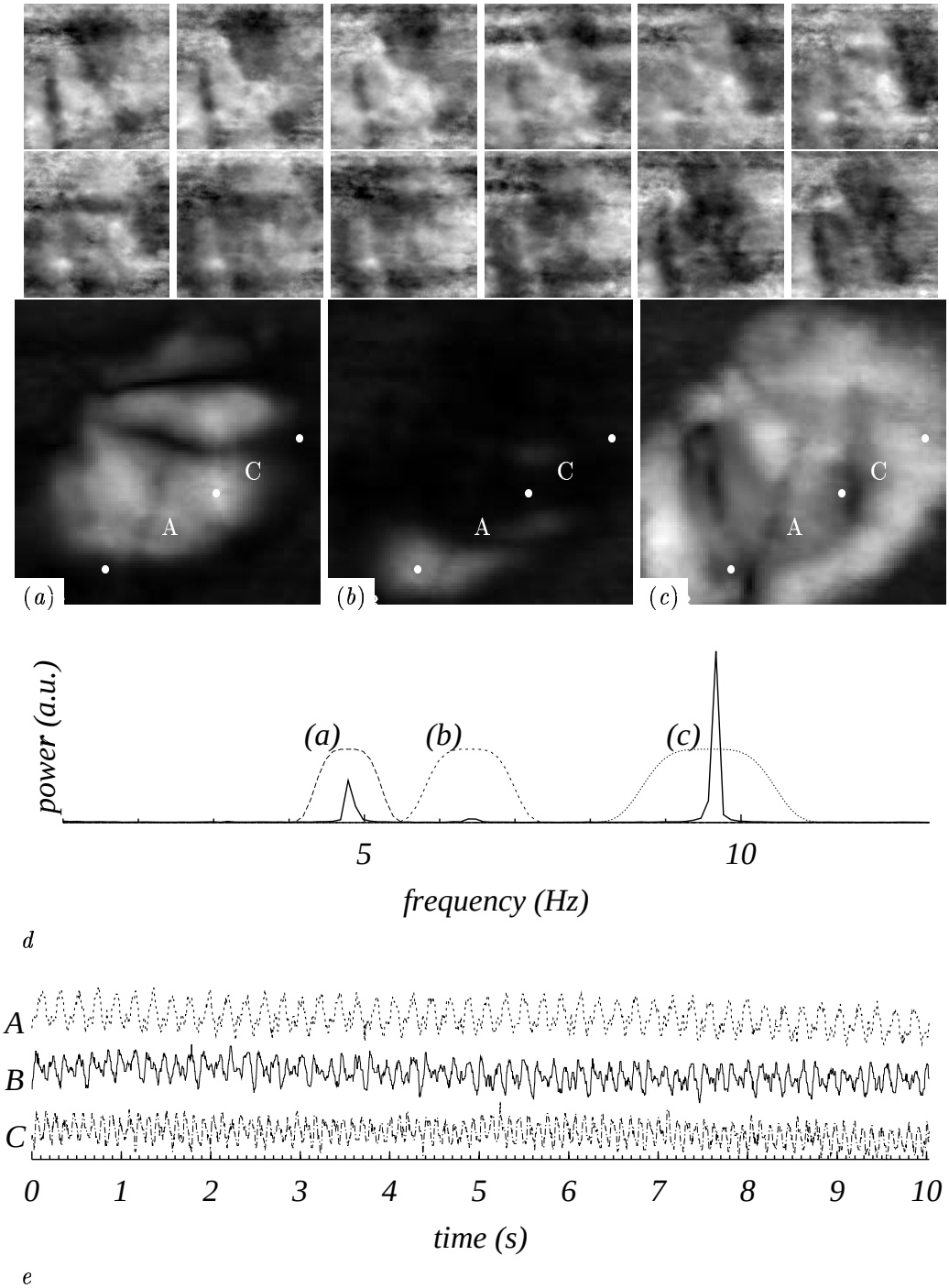


Figure 7: Dominant frequency domains in the experimental model of fibrillation. Top: 12 frames of the optical record of the epicardial activity, with interval 10 ms (left to right, top to bottom). Each frame represents square piece of the surface of approximately 3 cm size. $(a)$–$(c)$ Spatial distribution of the frequency components of the signal power. $(d)$ The cumulative power spectrum and the windows used to extract the frequency components shown. $(e)$ Signals recorded at points A, B and C designated on $(a)$–$(b)$. It is possible that domain $(c)$ (highest frequency) is synchronous with the re-entrant source, while two others to Wenckebach divided frequencies with ratios 1:2 and 2:3.

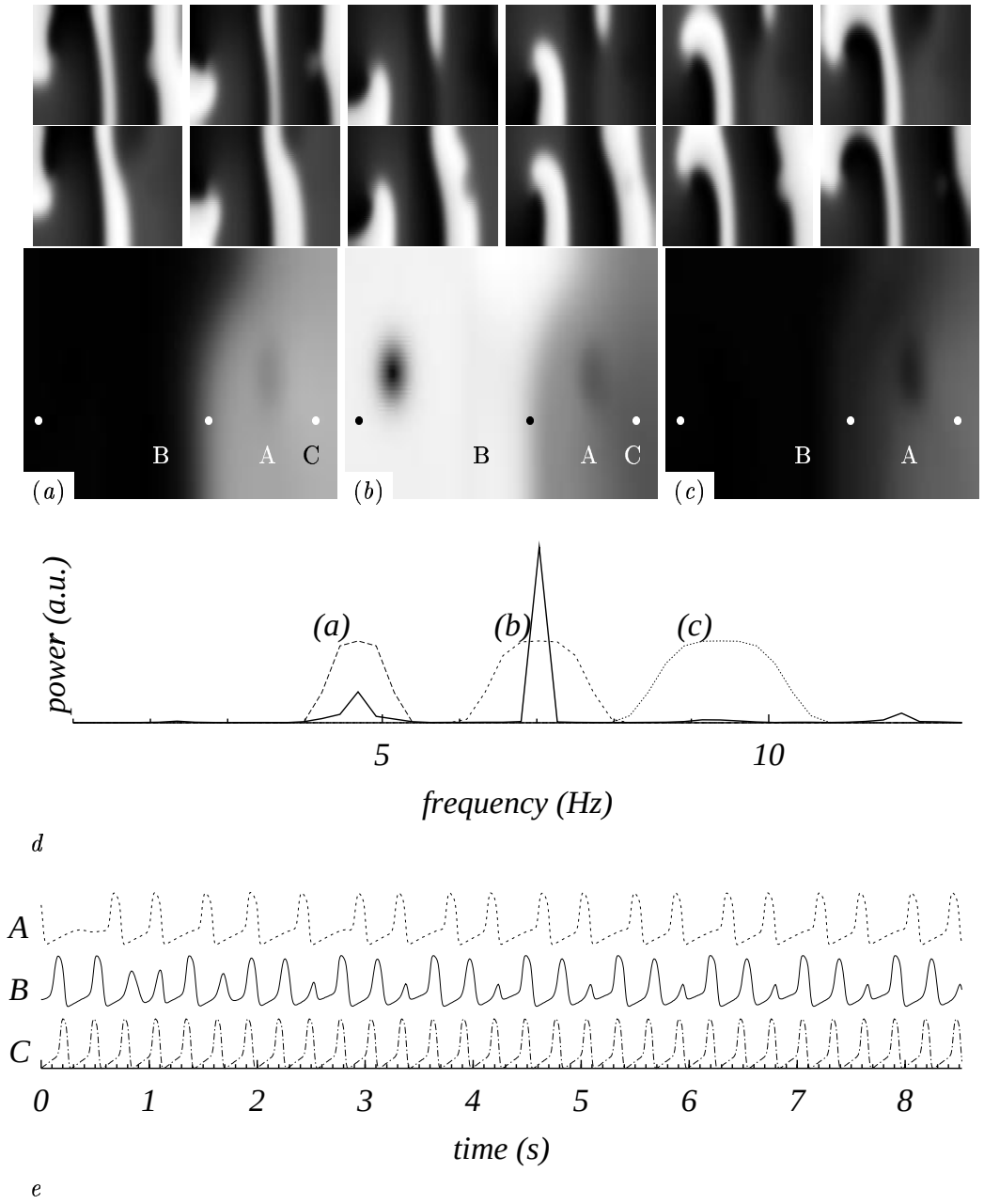


Figure 8: Dominant frequency domains in the numerical model of fibrillation (FHN). Top: 12 snapshots (stretch twice in vertical direction for visualisation purposes) of the activator distribution, with interval 2 t.u., conventionally equivalent to 25 ms (left to right, top to bottom). $(a)$–$(c)$ Spatial distribution of the frequency components of the signal power. $(d)$ The cumulative power spectrum and the windows used to extract the frequency components shown. $(e)$ Signals recorded at points A, B and C designated on $(a)$–$(b)$. Here the re-entrant source is in the left half of the medium, and corresponds to the medium frequency peak; the lower peak, represented in the right part of the medium, is 2:3 divided, and the higher peak is the higher harmonics of the lower peak.

control this source. To do that, the feedback protocol should be organised in such a way to monitor the rotation of the reentrant source, which is likely to be synchronous with the activity in the domain with fastest of the observed frequencies.

# References


[1] D. Noble. *Oxsoft HEART Version 3.8 manual.* Oxsoft, Oxford, 1990.

[2] R. FitzHugh. Impulses and physiological states in theoretical models of nerve membrane. *Biophysical Journal*, 1:445–466, 1961.

[3] A. T. Winfree. Varieties of spiral wave behaviour — an experimentalist's approach to the theory of excitable media. *Chaos*, 1:303–334, 1991.

[4] V. N. Biktashev and A. V. Holden. Control of re-entrant activity in a model of mammalian atrial tissue. *Proc. Roy. Soc. Lond. ser. B*, 260:211–217, 1995.

[5] V. N. Biktashev and A. V. Holden. Re-entrant activity and its control in a model of mammalian ventricular tissue. *Proc. Roy. Soc. Lond. ser. B*, 263:1373–1382, 1996.

[6] V. N. Biktashev, A. V. Holden, and H. Zhang. A model for the action of external current onto excitable tissue. *Int. J. of Bifurcation and Chaos*, 7:477–485, 1997.

[7] J. P. Keener. Direct activation and defibrillation of cardiac tissue. *J. Theor. Biol.*, 178:313–324, 1996.

[8] A. Pumir and V. Krinsky. How does an electric current defibrillate cardiac muscle. *Physica D*, 91:205–219, 1996.

[9] N. Trayanova, K. Scouibine, and F. Aguel. The role of cardiac tissue structure in defibrillation. *Chaos*, 8:221–233, 1998.

[10] E. Entcheva, J. Eason, I. R. Efimov, Y. Cheng, and R. and Malkin. Virtual electrode effects in transvenous defibrillation — modulationby structure and interface: Evidence from bidomain stimulations and optical mapping. *J. Cardiovasc. Electrophysiology*, 9:949–961, 1998.

[11] V. I. Krinsky, A. M. Pertsov, and V. N. Biktashev. Autowave approaches to cessation of reentrant arrhythmias. *Ann. N. Y. Acad. Sci.*, 591:232–246, 1990.

[12] K. I. Agladze, V. A. Davydov, and A. S. Mikhailov. Observation of a helical wave resonance in an excitable distributed medium. *JETP Letters*, 45:767–770, 1987.

[13] V. A. Davydov, V. S. Zykov, A. S. Mikhailov, and P. K. Brazhnik. Drift and resonance of spiral waves in active media. *Radiofizika*, 31:574–582, 1988.

[14] V. N. Biktashev and A. V. Holden. Design principles of a low-voltage cardiac defibrillator based on the effect of feed-back resonant drift. *J. Theor. Biol.*, 169:101–113, 1994.

[15] V. S. Zykov, A. S. Mikhailov, and S. C. Müller. Controlling spiral waves in confined geometries by global feedback. *Phys. Rev. Lett.*, 78:3398–3401, 1997.

[16] A. M. Pertsov, J. M. Davidenko, R. Salomonsz, W. Baxter, and J. Jalife. Spiral waves of excitation underlie reentrant activity in isolated cardiac muscle. *Circ. Res.*, 72:631–650, 1993.

[17] V. N. Biktashev, A. V. Holden, S. F. Mironov, A.M. Pertsov, and A.V. Zaitsev. Three dimensional aspects of re-entry in experimental and numerical models of ventricular fibrillation. *Int. J. of Bifurcation and Chaos*, 1999. to appear.

[18] A. V. Zaitsev, S. F. Mironov, O. Berenfeld, V. N. Biktashev, A. M. Pertsov, and J. Jalife. Domain organization of electrical activity during ventricular fibrillation in the isolated coronary perfused sheep ventricular muscle. *Circ. Res.*, 1999. in preparation.

[19] V. N. Biktashev, A. V. Holden, S. F. Mironov, A. M. Pertsov, and A. V. Zaitsev. On the mechanism of the domain structure of ventricular fibrillation. *Int. J. of Bifurcation and Chaos*, 1999. in preparation.

[20] V. N. Biktashev, A. V. Holden, S. F. Mironov, A. M. Pertsov, and A. V. Zaitsev. Two mechanisms of the domain structure of ventricular fibrillation. In *Physiological Society Abstracts, University College London Meeting*, Apr 1999.